# The crystal structure of thermally- and stress-induced Martensites in Ni2MnGa single crystals

V. Martynov, V. Kokorin

▶ **To cite this version:**

V. Martynov, V. Kokorin. The crystal structure of thermally- and stress-induced Martensites in Ni2MnGa single crystals. Journal de Physique III, 1992, 2 (5), pp.739-749. 10.1051/jp3:1992155 . jpa-00248778

**HAL Id: jpa-00248778**
**https://hal.science/jpa-00248778v1**

Submitted on 4 Feb 2008

**HAL** is a multi-disciplinary open access archive for the deposit and dissemination of scientific research documents, whether they are published or not. The documents may come from teaching and research institutions in France or abroad, or from public or private research centers.

L'archive ouverte pluridisciplinaire **HAL**, est destinée au dépôt et à la diffusion de documents scientifiques de niveau recherche, publiés ou non, émanant des établissements d'enseignement et de recherche français ou étrangers, des laboratoires publics ou privés.

Classification
*Physics Abstracts*
61.55Hg — 81.30K +

# The crystal structure of thermally- and stress-induced Martensites in $Ni_2MnGa$ single crystals

V. V. Martynov and V. V. Kokorin

Institute of Metal Physics, Academy of Sciences of Ukraine, Vernadskogo str. 36, 252680, Kiev-142, Ukraine

(*Received 13 September 1991, accepted 30 January 1992*)

**Abstract.** — Deformation behavior of $Ni_2MnGa$ single crystals uniaxially loaded in compression and tension along the $\langle 100\rangle$ $\beta_1$ and $\langle 110\rangle$ $\beta_1$ axes were investigated. It was shown that three successive stress-induced structural transitions may be observed for specimens tensed along the $\langle 100\rangle$ $\beta_1$ or compressed along the $\langle 110\rangle$ $\beta_1$ direction, while only one transition was stress-induced in compression along the $\langle 100\rangle$ $\beta_1$ axis. The crystal structure of stress-induced and thermal martensite was identified and related reversible deformation values for different loading geometry were estimated.

## 1. Introduction.

In the earlier investigations of $Ni_2MnGa$ intermetallic compound [1-2] it was shown, that in addition to the magnetic ordering, a structural phase transformation of martensitic type also took place during cooling. This martensitic transformation results in the formation of a complicated tetragonal lattice from b.c.c. ordered ($L2_1$) parent $\beta_1$ phase. From the combined powder diffraction and single-crystal X-ray analysis it was concluded, that apart from tetragonal distortion of $\beta_1$ phase there is also a superstructure with a periodicity along the $c$ axis of at least factor 4. The superstructure probably arises from stacking faults along the $c$ axis by a lattice shift in $\langle 110\rangle$ direction [1].

Recently it was shown [3] that the extra reflections, observed in X-ray diffraction patterns taken from the thermal martensite, were due to shuffling along the $(110)$ $[1\bar{1}0]_m$ system with a periodicity equal to 5 atomic layers. The same martensite was also stress-induced by compression along $\langle 100\rangle$ $\beta_1$ axis in the temperature range above $M_s$ temperature.

In the present article, we report the results on the deformation behavior of $Ni_2MnGa$ single crystals compressed/tensed along $\langle 100\rangle$ $\beta_1$ and $\langle 110\rangle$ $\beta_1$ axes in temperature range 308-77 K, and accompanied crystal structure changes, observed by *in situ* X-ray analysis. Origin of the extra spots in X-ray patterns, and relations between the macroscopic deformations and corresponding lattices parameters changes are also discussed.

## 2. Materials and experimental technique.

The alloy used for the investigations was melted in induction melting furnace in an argon atmosphere. $Ni_2MnGa$ single crystals were grown according to Bridgman's technique without

using seeding crystals. Samples of square cross-section having the dimensions $1 \times 1 \times 12$ mm$^3$ were used for four-point probe resistivity measurement, though for mechanical testing experiments and X-ray analysis the specimens used were of circular cross-section with « heads » on its ends. Because of high brittleness of $Ni_2MnGa$ these specimens were made as compound (Fig. 1), consisting of electropolished cylindrical $Ni_2MnGa$ single crystal rod and brass « heads », soldered to it by tin solder. The gauge length of these specimens were 2.0 mm for compression experiments and 4-10 mm for tension ones. Mechanical tests were performed using ZM-40 mechanical testing machine, adjusted for compression and tension of micro specimens. Temperature stabilization for isothermal tension and compression experiments was achieved by immersing specimens in Dewar vessel filled with water or petrol for the experiments carried above or below zero temperature respectively. For crystal structure analysis the *in situ* X-ray rotating and oscillating single-crystal methods performed at room temperature were used.

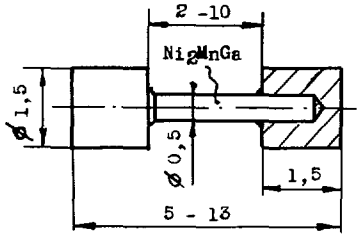


Fig. 1. — *Composed specimen for compression and tension experiments.*

### 3. Results and discussion.

Figure 2 shows typical resistivity curve for single crystals used in experiment. Characteristic points for thermally-induced martensitic transformation were found to be : $M_s = 293$ K, $M_f = 273$ K, $A_s = 278$ K, $A_f = 298$ K with a small scattering (about $\pm 5$ K) around these values due to composition inhomogeneity. Measured lattice parameter of $L2_1$ ordered $\beta_1$ phase was established to be $0.5822 \pm 0.0002$ nm. (It is necessary to point out, that due to closeness of atomic scattering factors of constituent elements the superstructure reflections due to $L2_1$ ordering cannot be resolved and only diffraction spots of A2 crystal structure are present at the X-ray diffraction patterns.)

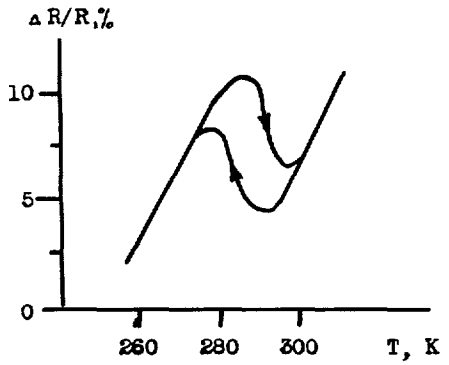


Fig. 2. — Resistivity changes in $Ni_2MnGa$ single crystal during cooling and heating.

The crystal structure of thermally-induced martensite may be interpreted in terms of tetragonal body centered lattice having the lattice parameters $a = b = 0.590 \pm 0.001$ nm, $c = 0.554 \pm 0.001$ nm. However except the strong spots due to b.c.t. lattice, relatively weak additional reflections are also observed at X-ray oscillation patterns taken from the thermally-induced martensite (Fig. 3). As it has already been pointed out [3], all these additional spots are situated along reciprocal lattice rows which are parallel to one of two $\langle 110 \rangle_m$ direction and divide the distance between the main b.c.t. spots into 5 equal parts. If one denotes the intensity of the main spots as « strong » (S), then additional four spots may be divided into two groups having the intensities « mediate » (M) and « weak » (W) correspondingly (see Fig. 3b). Absolute intensity values of additional spots depend upon the indices of particular reciprocal row, however, the above mentioned intensity distribution is valid for all of them.

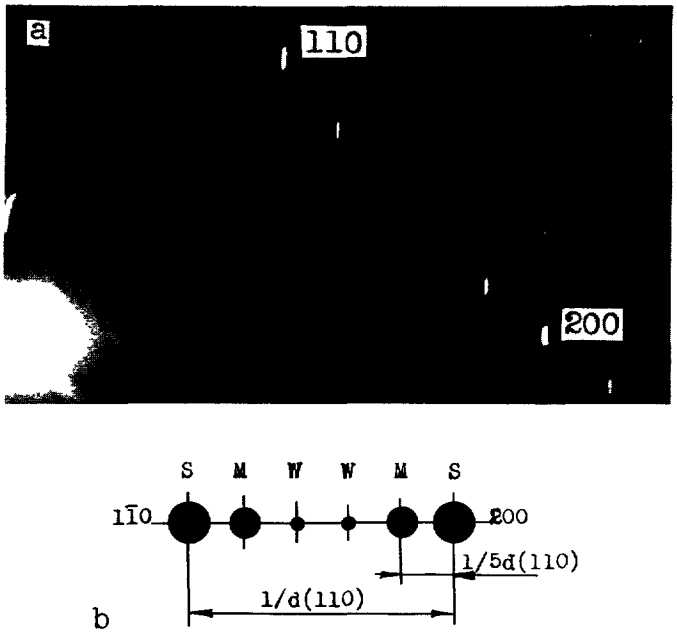


Fig. 3. — X-ray oscillation pattern for thermally-induced martensite (a) and key diagram for the $\langle 110 \rangle_m$ relrow (b).

From the analysis of additional reflections absence and diffraction angles of the main b.c.t. lattice reflections one may conclude that additional maxima are the result of periodical shuffling (modulation) along (110) [1$\bar{1}$0] system of b.c.t. martensite in such a way that each 5-th $(110)_m$ plane remains in its original (i.e. b.c.t.) position (Fig. 4). The sign and magnitude of displacements for each (110) plane along the modulation period may be evaluated from the experimentally measured intensity distribution between the additional maxima and calculated intensity for different modes of 5-layer modulation.

Structure factor for a given $hk\ell$ plane in coordinate system $x$, $y$, $z$ for nonprimitive cells may be written as

$$F_{hk\ell} = F_0 \sum_{j=1}^{N} \exp 2\pi i (hx_j + ky_j + \ell z_j),$$

where $F_0$ is the structural factor for a plane net of atoms, $N$ is a number of such nets in the structural period along the normal to the net plane, $x_j$, $y_j$, $z_j$ are the coordinates of the $j$-th net, expressed as the fractions of the corresponding identity periods. For example, if (110) plane is chosen as the atom net for any body centered lattice with the parameters $a$, $b$ and $c$, than for the coordinate system $x \parallel [1\bar{1}0]$, $y \parallel [001]$, $z \parallel [110]$ structural factor will be given by

$$F_{hk\ell} = F_{110} \sum_{j=1}^{2} \exp 2\,\pi i \left( h\frac{j}{2} + \ell\frac{j}{2} \right),$$

where $h$, $k$, $\ell$ are the indices of reflections in orthogonal coordinate axes having the following translation periods : $a' = c' = \sqrt{a^2 + b^2}$, $b' = c$.

For the shuffling along the (110) $[1\bar{1}0]$ system with the number of layers in the modulation period equal to $L$, the structural factor for the odd $L$ is written as

$$F_{hk\ell} = F_{110} \sum_{j=1}^{2L} \exp 2\,\pi i\,[h(j/2 + \Delta_j) + \ell j/2\,L]\,,$$

where $\Delta_j$ is displacement of $j$-th plane from the regular position in shuffling direction (Fig. 4)

$$\Delta_j = A \sin 2\,\pi j/L + B \sin 4\,\pi j/L + C \sin 6\,\pi j/L\,.$$

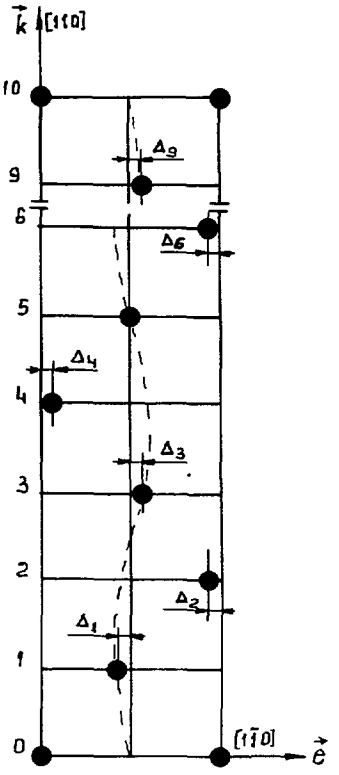


Fig. 4. — Projection of 5-layer modulated structure onto (010) plane.

Constants $A$, $B$ and $C$ were selected according to the least discrepancy between the experimentally measured intensities ($I$) of the main and additional spots situated along [110] b.c.t. (20 $\ell$ in the « new » $x$, $y$, $z$ axes) direction and corresponding calculated $(F_{20\ell})^2$ values. Measured relative intensities for thermally-induced 5-layer martensite ($I$) and corresponding calculated $(F)^2$ values for the particular constants $A = -0.06$, $B = 0.002$, $C = -0.007$ are listed in the table I. Thus, the shear modulation of b.c.t. martensite lattice may be considered as superimposed static displacement waves having the following propagation and polarization vectors : $\mathbf{k}_{1,2,3} \| [110]$, $\mathbf{e}_{1,2,3} \| [1\bar{1}0]$, $|\mathbf{k}_1| = 4\ \pi/5\ a\sqrt{2}$, $|\mathbf{k}_2| = 8\ \pi/5\ a\sqrt{2}$, $|\mathbf{k}_3| = 12\ \pi/5\ a\sqrt{2}$, $|\mathbf{e}_1| \cong a\sqrt{2}/17$, $|\mathbf{e}_2| \cong a\sqrt{2}/500$, $|\mathbf{e}_3| = a\sqrt{2}/150$.

The first series of deformation experiments was performed using specimens loaded in compression. Figure 5 shows stress-strain (s-s) curves obtained at different temperatures during isothermal compression along the $\langle 100 \rangle\ \beta_1$ axis. For this particular compression

Table I. *Measured* ($I_m$) *and calculated* ($|F|^2$) *intensities values for 5-layer modulated martensite.*

| $hk\ell$ | $I_m$ | $\|F\|^2$ |
|---|---|---|
| 200 | 74 | 74.12 |
| 202 | 14 | 13.98 |
| 204 | < 1 | < 0.01 |
| 206 | < 1 | 1.08 |
| 208 | 11 | 10.82 |

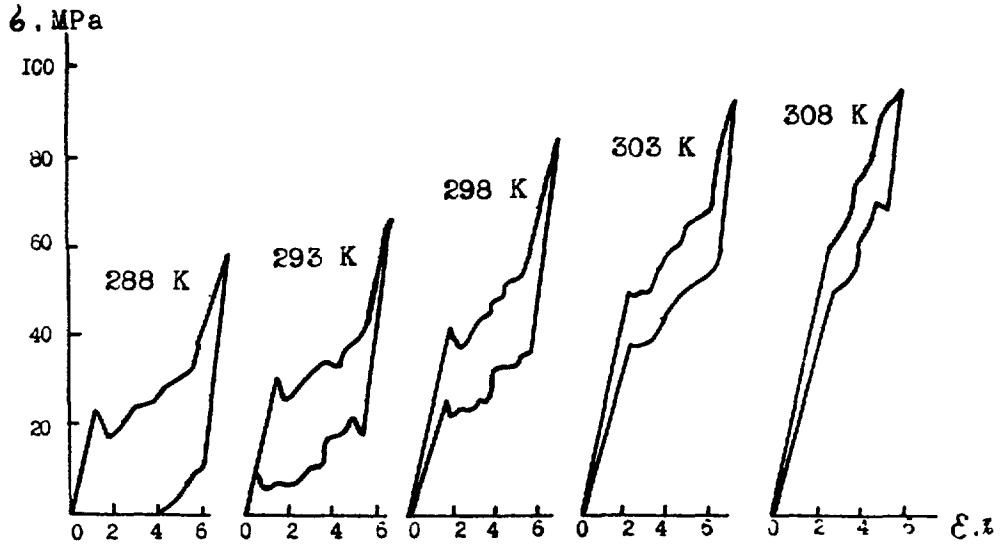


Fig. 5. — Stress-strain curves for compression along the $\langle 100 \rangle\ \beta_1$ axis.

direction the maximum contraction value, corresponding to martensite formation in the whole specimen volume (~ 5 %), and the character of s-s curves remain unchanged even for specimens loaded up to destruction. It also can be seen, that in temperature range above 293 K deformation is fully reversible. Stress, necessary for stress-induced martensite formation linearly follows the deformation temperature, $d\sigma/dT \cong 2.5$ MPaK$^{-1}$.

Principally different s-s curves were obtained for compression along the $\langle 110 \rangle$ $\beta_1$ direction. In contrast with the previous case here more than one deformation stage are usually obtained in s-s curves, the number of stages being dependent on the deformation temperature (Fig. 6). For example, at 279 K compression proceeds in three distinct stages, while unloading consists of only two ones, indicating that part of the deformation, accumulated during the first deformation stage, is stable at this temperature (dashed line is the beginning of s-s curve for the second and following deformation cycles). Lowering of the deformation temperature results in reducing the number of stages at unloading branch of s-s curve. It can be seen, that in temperature range 243-213 K only one-stage unloading branch is observed and below 193 K all deformation is irreversible (complete restoration of initial dimensions was always observed upon heating to the room temperature). The stress level, necessary for starting any deformation stage, decreases when the deformation temperature decreases, the maximum deformation, accumulated during compression along $\langle 110 \rangle$ $\beta_1$ axis, is about 4 %. It is worth to point out that at 289 K both contraction on loading and elongation upon releasing of the

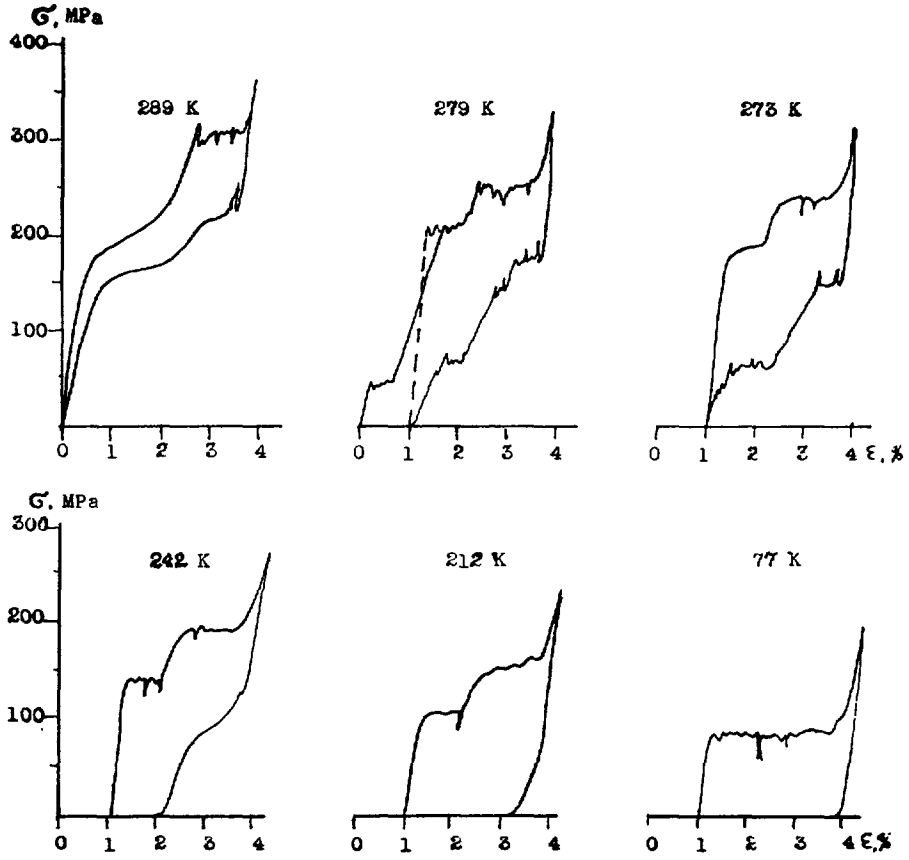


Fig. 6. — Stress-strain curves for compression along the $\langle 110 \rangle$ $\beta_1$ axis.

load proceed in only two stages (see Fig. 6), while attained deformation value is also about 4 %. Here the deformation value, attained during the first deformation stage is equal to the sum of the two first deformation stages of three-stage curves, observed at lower temperatures.

Results very similar to those described above were also observed for tension along the $\langle 100 \rangle$ $\beta_1$ direction (Fig. 7). One can see that significantly lower tensile stress levels, necessary for beginning of corresponding deformation stages, and larger values of deformations, attained at each stage, are obtained in the tension experiments.

Macroscopic observations of polished specimens surface during loading show that at the beginning of each deformation step one or more thin parallel layers crossing the specimen initially arise. As the deformation proceeds they become thicker and, new layers appear in different parts of the specimen. At the end of corresponding stage, all of them coalesce together, forming new contrast over the whole specimen length. Upon unloading reverse processes takes place.

All these results, namely : deformation reversibility (either upon unloading or during subsequent heating) ; fixed deformation values for each stage ; temperature dependence of necessary stress level for step formation at s-s curve ; specimens surface contrast evolution during deformation — allow to suppose that each deformation stage corresponds to stress-induced structural phase transition.

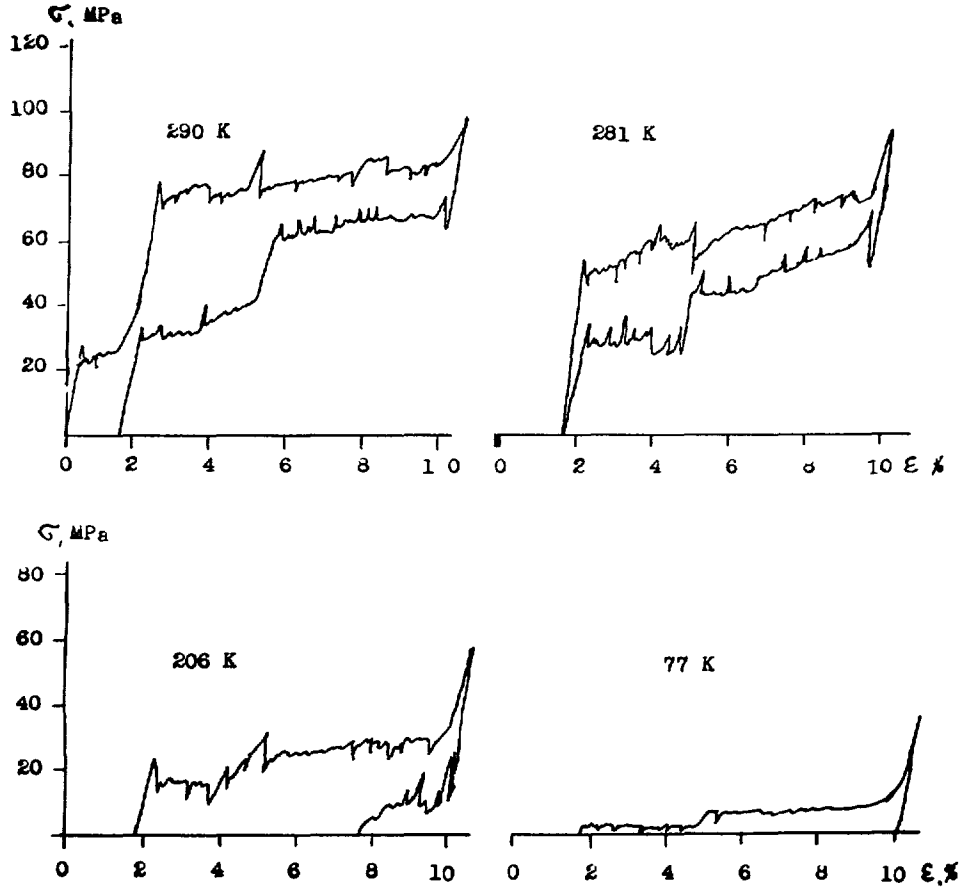


Fig. 7. — Stress-strain curves for tension along the $\langle 100 \rangle$ $\beta_1$ axis.

The experimental technique used in the present experiments allowed to make *in-situ* X-ray analysis only at room temperature (~ 290 K). For the specimens used, this particular temperature corresponds to one-step loading curve for the compression along the $\langle 100\rangle\ \beta_1$ direction (see Fig. 5), two-step one for the compression along the $\langle 110\rangle\ \beta_1$ direction (see Fig. 6) and the three-steps loading s-s curve for the tension along the $\langle 100\rangle\ \beta_1$ axis (see Fig. 7). So it enables to make structural analysis of all changes which take place at different stages during compression and tension.

As it has already been reported [3], the main diffraction spots of X-ray patterns taken from stress-induced martensite formed during compression along $\langle 100\rangle\ \beta_1$ axis correspond to single crystal of b.c.t. martensite with its *c* axis parallel to the compression direction. Analysis of relative positions and intensity of additional (weak) spots leads to the conclusion that crystal structure of stress-induced martensite is completely identical to the thermally-induced one described above.

The same b.c.t. martensite having the 5-layers modulation is also formed at the first deformation stage in specimens oriented along $\langle 100\rangle\ \beta_1$ and loaded in tension. Further increase of the load results in formation of new crystal structure, which differs from the previous one in symmetry and modulation period length. Additional diffraction spots, which also lie in $\langle 110\rangle_m$ direction, now divide the distance between the main spots of orthorhombic lattice into 7 equal parts (Fig. 8). According to the main (strong) diffraction spots, the crystal lattice of this stress-induced phase may be regarded as body centered orthorhombic having parameters $a = 0.612 \pm 0.001$ nm, $b = 0.578 \pm 0.001$ nm, $c = 0.554 \pm 0.001$ nm, with the *a* axis along the tensile direction. Using the above described approach for evaluation of modulation parameters one can found that experimentally observed intensity distribution for 7-layer modulation can be described by $A = 0.083$, $B = -0.027$, C=0. Measured and calculated intensities for 20 $\ell$ relrow of orthorhombic lattice are listed in table II. In this case modulation may be regarded as two superimposed static waves of share displacements : $\mathbf{k}_{1,2} \| [110]$, $\mathbf{e}_{1,2} \| [1\bar{1}0]$, $|\mathbf{k}_1| = 4\ \pi/7\ a\sqrt{2}$, $|\mathbf{k}_2| = 8\ \pi/7\ a\sqrt{2}$, $|\mathbf{e}_1| \cong a\sqrt{2}/12$, $|\mathbf{e}_2| \cong a\sqrt{2}/40$.

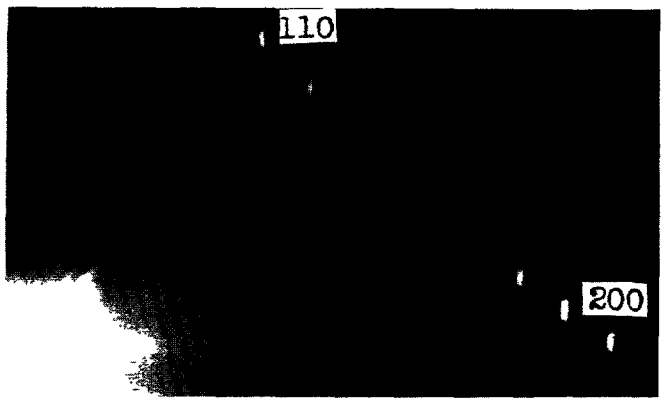


Fig. 8. — X-ray oscillating pattern for stress-induced 7-layer modulated martensite.

Stress-induced b.c.t. and orthorhombic martensite formation are also observed during compression along the $\langle 110\rangle\ \beta_1$ direction, however in the last case *a* axes are normal to the compression direction. It is worth to be mentioned that at 289 K compression along the $\langle 110\rangle\ \beta_1$ direction results in direct formation of orthorhombic 7-layer modulated martensite

Table II. *Measured* ($I_m$) *and calculated* ($|F|^2$) *intensity values for 7-layer modulated martensite.*

| $hk\ell$ | $I_m$ | $\|F\|^2$ |
|---|---|---|
| 200 | 51 | 52.40 |
| 202 | 23 | 27.34 |
| 204 | $< 1$ | $\sim 0.01$ |
| 206 | $< 1$ | 0.07 |
| 208 | $\sim 1$ | 0.96 |
| 2 010 | 7 | 6.25 |
| 2 012 | 18 | 12.96 |

from the initial $\beta_1$ phase ; this fact explains the relatively large deformation value, observed at the first deformation stage of s-s curve taken at this temperature. (Similar two-stage s-s curve having extended first deformation stage were also observed at 303 K for tension along $\langle 100 \rangle$ $\beta_1$ direction.)

After the orthorhombic martensite is formed in the whole specimen volume, further tension along the $\langle 100 \rangle$ $\beta_1$ direction or compression along the $\langle 110 \rangle$ $\beta_1$ direction results in one more stress-induced structural transition. X-ray patterns taken from crystals formed, show disappearance of additional spots due to share modulation and indicate that new b.c.t. crystal structure is formed. In contrast with the 5-layer modulated b.c.t. phase, having $c/a < 1$, newly formed b.c.t. martensite possesses tetragonality $c/a > 1$. Measured parameters of this phase are $a = b = 0.552 \pm 0.001$ nm, $c = 0.644 \pm 0.001$ nm, $c$ axis is along the tensile axis or normal to the compression one.

The lattice parameters ($a_i$, $i = 1, 2, 3$) of the parent $\beta_1$ phase and of three successively formed martensites designated for convenience as $\beta_1'$, $\beta_1''$ and $\beta_1'''$ are listed in the table III. (Data, listed in the same rows of the table, represent the axes which maintain correspondence

Table III. *Lattice parameters of parent* $\beta_1$ *and martensite* $\beta_1'$, $\beta_1''$ *and* $\beta_1'''$ *phases.*

| Axes | Lattice parameters, nm | | | |
|---|---|---|---|---|
| | $\beta_1$ | $\beta_1'$ | $\beta_1''$ | $\beta_1'''$ |
| $a_1$ | 0.5824 | 0.590 | 0.612 | 0.644 |
| $a_2$ | 0.5824 | 0.590 | 0.578 | 0.552 |
| $a_3$ | 0.5824 | 0.554 | 0.554 | 0.552 |

during successive $\beta_1 \rightarrow \beta_1' \rightarrow \beta_1'' \rightarrow \beta_1'''$ phase transformations.) Using these values for calculation principal strains, the deformation tensors can be written for each phase transition :

$$E_{\beta_1 - \beta_1'} = \begin{pmatrix} 0.013 & 0 & 0 \\ 0 & 0.013 & 0 \\ 0 & 0 & -0.049 \end{pmatrix}, \quad E_{\beta_1' - \beta_1''} = \begin{pmatrix} 0.037 & 0 & 0 \\ 0 & -0.02 & 0 \\ 0 & 0 & 0 \end{pmatrix},$$

$$E_{\beta_1'' - \beta_1'''} = \begin{pmatrix} 0.052 & 0 & 0 \\ 0 & -0.045 & 0 \\ 0 & 0 & -0.003 \end{pmatrix}.$$

From these expressions upper limit of attained deformation value due to corresponding transformation ($\varepsilon$) for the predetermined direction can be obtained $\varepsilon = \varepsilon_i \ell_i$, where $\varepsilon_i$ are the principal strains, $\ell_i$ are directional cosines. Stress-induced transformation under tension or compression will take place only when the product of applied normal stress $\sigma$ ($\sigma > 0$ for tension, $\sigma < 0$ for compression) and deformation in the direction of acting force $\varepsilon$ ($\varepsilon > 0$ for elongation, $\varepsilon < 0$ for contraction) is of positive sign $\sigma\varepsilon > 0$. It is obvious that for tension along the $\langle 100 \rangle$ $\beta_1$ direction ($\ell_1 = 1$, $\ell_2 = \ell_3 = 0$) there is such a variant of martensites orientation for which $\sigma\varepsilon > 0$ for the whole sequence of phase transitions. For this case calculated elongations are :

$$\varepsilon^{t\langle 100 \rangle}_{\beta_1 - \beta_1'} = 0.013\,, \quad \varepsilon^{t\langle 100 \rangle}_{\beta_1' - \beta_1''} = 0.037\,, \quad \varepsilon^{t\langle 100 \rangle}_{\beta_1'' - \beta_1'''} = 0.052\,,$$

and all of them are in a good agreement with the experimental data (see Fig. 7). The same conclusion concerning the possibility of the whole sequence of phase transitions is also valid for compression along the $\langle 110 \rangle$ $\beta_1$ direction ($\ell_1 = 0$, $\ell_2 = \ell_3 = \sqrt{2}/2$). Corresponding contractions are :

$$\varepsilon^{c\langle 110 \rangle}_{\beta_1 - \beta_1'} = -0.018\,, \quad \varepsilon^{c\langle 110 \rangle}_{\beta_1' - \beta_1''} = -0.01\,, \quad \varepsilon^{c\langle 110 \rangle}_{\beta_1'' - \beta_1'''} = -0.024\,,$$

as compared with $\sim 2$ %, $\sim 1$ % and $\sim 2$ % taken from compression experiments for these transitions. However for compression along $\langle 100 \rangle$ $\beta_1$ direction $\sigma\varepsilon > 0$ is valid only for the first and the third phase transitions :

$$\varepsilon^{c\langle 100 \rangle}_{\beta_1 - \beta_1'} = -0.049\,, \quad \varepsilon^{c\langle 100 \rangle}_{\beta_1' - \beta_1''} = 0\,, \quad \varepsilon^{c\langle 100 \rangle}_{\beta_1'' - \beta_1'''} = -0.003\,.$$

In the last case the contraction value is very small and apparently the necessary stress level for stress-induced transformation is too high to be achieved before breaking of the specimen.

## 4. Conclusions.

a) Three $\beta_1'$, $\beta_1''$ and $\beta_1'''$ martensites were observed in $Ni_2MnGa$ single crystals. The parent-to-martensite $\beta_1 \rightarrow \beta_1'$ phase transition can be both thermally-induced by cooling to $M_s$ point and stress-induced in temperature range above $M_s$, while $\beta_1' \rightarrow \beta_1''$ and $\beta_1'' \rightarrow \beta_1'''$ martensite-to-martensite transitions can be only stress-induced by properly oriented external stress both below and above $M_s$.

b) Stress level which is necessary for all stress-induced transformations decreases with lowering of deformation temperature. Once formed $\beta_1'$, $\beta_1''$ and $\beta_1'''$ phases are stable below 298 K, 233 K and 193 K respectively. Contraction and elongation values calculated from the lattice parameters of corresponding phases are in a good agreement with experimental results.

c) It was shown that formation of $\beta_1'$ and $\beta_1''$ phases is accompanied with additional shuffling (besides the lattice distortion) which may be regarded as static wave of shear

displacements along (110) $[1\bar{1}0]$ system. The wave length for $\beta_1'$ and $\beta_1''$ phases are $5\,a\sqrt{2}$ and $7\,a\sqrt{2}$ respectively, the maximum displacement of (110) planes from their original positions is about $a\sqrt{2}/10$.

**Acknowledgments.**

The authors are grateful to Yu. V. Martynov for his assistance in making computer program for modulated structures parameters calculation.

## References

[1] WEBSTER P. J., ZIEBECK K. R. A., TOWN S. L., PEAK M. S., Magnetic order and phase transformation in $Ni_2MnGa$, *Philos. Mag.* **49** (1984) 295-310.

[2] KOKORIN V. V., OSIPENKO I. A., SHIRINA T. V., Phase transformation in $Ni_2MnGa_{\varepsilon}$. Fiz. Met. Metalloved. **67** (1989) 601-603.

[3] ZASIMCHUK I. K., KOKORIN V. V., MARTYNOV V. V., TKACHENKO A. V., CHERNENKO V. A., Martensite crystal structure in $Ni_2MnGa$ alloy. Fiz. Met. Metalloved. (1990) 110-114.